Astron. Astrophys. 324, 435–448 (1997)

ASTRONOMY
AND
ASTROPHYSICS

Chemical composition of six K supergiants in the Small Magellanic Cloud⋆

V. Hill

Observatoire de Paris, Section de Meudon, DASGAL, URA 335 du CNRS, F-92195 Meudon Cedex, France

Received 12 August 1996 / Accepted 25 September 1996

Abstract. A sample of six SMC cool stars (K supergiants) are analysed by high resolution spectroscopy in order to investigate their chemical content, which should reflect that of the current interstellar medium within the SMC. The abundance of Na, Al, α-elements, Fe peak and heavy elements are derived through an LTE analysis of the lines, compared to a Galactic "standard" (the well-studied K giant Arcturus) and discussed in terms of chemical evolution of the SMC. The following results were obtained: 1.) All the stars from this sample are metal deficient ([Fe/H] ranges from –0.59 to –0.89 dex). The abundance varies little from star-to-star (0.10 dex rms, comparable with the expected error due to uncertainties on the effective parameters of the stars), in agreement with the very small chemical composition variations among the H II regions within the SMC found by Pagel et al. 1978. 2.) Sodium is not strongly enhanced in these stars, and the star-to-star scatter is larger than expected. 3.) At variance with metal-poor stars in our Galaxy, the so-called α-elements do not seem to be enhanced. 4.) Nickel displays a noticeable depletion with respect to iron ([Ni/Fe]$\approx$–0.3 dex), at variance with what is found in the SMC F supergiants and in Arcturus. 5.) Except for PMMR 144, the *s* and *r* process elements heavier than Ba are enhanced in all of our stars by $\simeq$+0.4 dex.

Key words: stars: abundances – stars: supergiants – galaxies: Magellanic Clouds – galaxies: abundances

1. Introduction

The Magellanic Clouds have often been used as laboratories to test the validity of theories built up in our own Galaxy. In particular, the understanding of the chemical evolution of these two galaxies is of great interest as a probe of evolution of extragalactic systems. From numerous metallicity indicators, the present day metallicity of the Clouds have been determined to be around half solar ([M/H]$\simeq$-0.25 dex) and one fifth of solar ([M/H]$\simeq$-0.7 dex) respectively in the Large and Small Magellanic Cloud, implying that the Magellanic Clouds have not evolved at the same rate as our own Galaxy.

In the last years, modern detectors have made it possible to observe high resolution spectra of luminous young stars, providing information on the chemical content of these stars (abundances of numerous elements). The latest studies concerned F supergiant stars (Russell and Bessell 1989, hereafter RB89; Spite et al. 1989, hereafter SSF89; Luck and Lambert 1992, hereafter LL92; Hill et al. 1995). Studies of H II regions (Pagel 1978, Dufour 1984, Russell & Dopita 1992 and references therein) also give information on the abundance of the lighter elements (C,N,O, S, etc.). The general findings from these studies is that the abundance pattern of the elements do not always follow the solar pattern, in particular concerning the light elements and the neutron capture elements, which are not yet fully understood. Moreover, in the Small Magellanic Cloud (SMC), from the F stars studies, it is not very clear whether the abundances are homogeneous across the whole galaxy or if a dispersion, exists. Confusing also, was the finding that the young cluster NGC330 appeared to be noticeably more metal poor than its surroundings (Spite et al. 1991).
Since deriving abundances in very luminous stars is always questionable because of the extreme atmospheres that are concerned (non-LTE effects are almost surely present), it appeared useful to study also a slightly different kind of cooler stars: the K supergiants, in particular to be used as field "reference stars" for a future analysis of a more complete sample of stars in NGC 330. Furthermore, state of the art models specifically developed for cool giants stars were made available by B. Plez (1992 and 1995) and made it possible to derive precise abundances from these metal-poor K supergiants.
In this paper, we present the analysis of six K supergiant stars of the SMC. The abundances of 16 elements from sodium to europium are derived and discussed in terms of chemical evolution of the galaxy. The scatter around the mean value for our sample is also discussed in terms of homogeneity of the SMC. The abundance of C, N and O will be discussed in a forthcoming paper by Hill & Barbuy (1996).

⋆ Based on observations collected at the European Southern Observatory, La Silla, Chile.

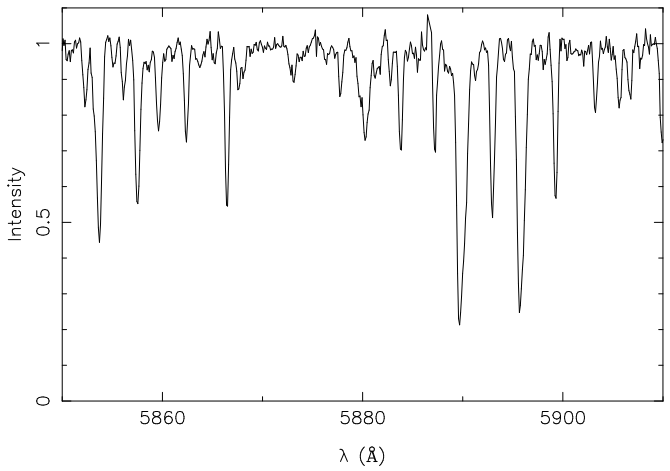

Fig. 1. Order number 97 of the reduced echelle-spectrum of the star PMMR 145

2. Observations

2.1. Choice of the sample stars

The six stars were chosen from the Prévot et al. 1983 catalogue (hereafter PMMR) of red stars with similar $(B-V)$ colors (ranging from 1.6 to 1.8); on the other hand, they were chosen to be widely spread out over the Small Magellanic Cloud in order to be able to check the homogeneity of the chemical composition of stars in various regions of the Cloud.

The observations were carried out from 1989 to 1993, first as a part of the ESO "Magellanic Clouds" key-program, and during subsequent observations, using either the EMMI spectrometer fed by the New Technology Telescope (NTT) or the CASPEC fed by the 3.6m telescope at ESO La Silla (Chile). The log book of the observations is presented in Table 1. The spectra obtained with EMMI have a resolving power of ≈30000 and those obtained with CASPEC of ≈20000, and the signal to noise ratio was of 100 on average. For each star, we obtained two overlapping echelle spectra in order to cover a large spectral range, and the overlapping region was used to reduce the stochastic errors on the equivalent width of the spectral lines by averaging the measurements from the two spectra.
The spectra were reduced using a semi-automatic code especially developed by Spite (1990) which finds and extracts the spectral orders (optimal extraction), performs flat fielding and wavelength calibration from the comparison lamp spectrum and computes the radial velocity. An example of a reduced spectrum is given in Fig 1.

3. Analysis

The model atmospheres that we used to derive the abundances were interpolated in Plez's (1992, and 1995) grid of models, which code is adapted from the MARCS'. With temperature and gravity ranges ($3500 \leq T_{eff} \leq 4750$ K and $-0.5 \leq \log g \leq 1.0$ dex) for metallicities from –0.6 dex to +0.6 dex and taking into account the sphericity effect these model were especially developed to represent the atmosphere of K giants. This grid is therefore perfectly well suited for metal-poor K supergiant stars in the Magellanic Clouds.

For the abundance analysis of our K supergiant stars, we chose to restrict ourselves to the relatively weak lines : below the the saturation of the curve of growth (which corresponds to equivalent widths of the order of 150 to 200 mÅ) the abundance deduced from the lines are very little dependent upon the microturbulent velocity (v_t). Since this parameter is not very well known in these stars, we only took into account the abundances calculated from lines with W $\leq$ 200 mÅ.

After this selection we were left with (for each star) 28 to 77 Fe I lines, 7 to 11 Fe II lines, 7 to 23 Ti I lines, 8 to 16 Ni I lines, and a few lines of each other species.

The oscillator strengths of the lines were calculated from the inverse analysis of the solar spectrum using the Holweger-Müller (1974) solar model. The solar abundances were taken from Grevesse & Noels (1993). For most lines, we determined equivalent widths by the Gaussian approximation and deduced the abundances from this measurement. However, when the lines were severely blended, or affected by fine or hyperfine structure (FS or HFS), a synthetic spectrum was computed over several Å and compared to the observed one. The data for the hyperfine structure (for elements such as Sc, Mg and Eu) were taken from Steffen (1985). In these cool stars, the light elements (carbon, nitrogen and oxygen) are partly locked in molecules (CN, CO, C_2), so their abundance will be determined using molecular synthetic spectra and discussed in a forthcoming paper. A complete list of the lines used together with their excitation potential and oscillator strength can be found in the Appendix.

3.1. Effective parameters determination

The effective parameters of the stars were determined by an iterative process on effective temperature (T_{eff}), gravity ($\log g$), microturbulent velocity (v_t) and metallicity ([M/H]).

– **Effective temperature**
we used as a first guess the T_{eff} derived from the confrontation of the observed $(B-V)$ colors and those calculated from Plez' model (Plez 1995). The individual reddenings for each stars were not available, so we took the mean reddening (averaged over 40 SMC stars) from Grieve & Madore (1986). Since both the photometry and the reddenings available are of rather poor quality for these stars (the aperture photometry may be questionable because of possible crowding effects), this temperature was only used as a starting-point for the analysis, and was given no further weight in the final effective temperature adopted. The method to determine the temperature thus mainly relied on the excitation equilibrium method, asking that lines of a same species with high and low excitation potential should produce the same abundance. This method was applied to Fe I lines with W $\leq$ 200 mÅto determine T_{eff} for all our stars. The expected intrinsic uncertainty on the determination of effective temperature by this method should be $\leq \pm 200$ K

Table 1. Logbook of the observations

star	V	$(B-V)$	Date	Instrument	$\Delta\lambda(nm)$	V_r (kms^{-1})
PMMR 23	12.42	1.81	Dec 92	EMMI	500-630	137.7
PMMR 23			Dec 92	EMMI	620-720	-
PMMR 27	13.2	-	Dec 93	EMMI	580-690	156.4
PMMR 48	12.7	-	Dec 93	EMMI	570-680	156.1
PMMR 48			Dec 93	EMMI	580-700	156.1
PMMR 102	12.87	1.60	Oct 91	EMMI	500-630	163.1
PMMR 102			Oct 91	CASPEC	530-670	161.6
PMMR 144	12.82	1.10	Dec 93	EMMI	580-670	179.0
PMMR 144			Dec 89	CASPEC	590-680	180.4
PMMR 145	13.09	1.59	Oct 91	EMMI	500-630	159.3
PMMR 145			Dec 93	EMMI	590-690	160.6

The magnitude and colors for the stars are from Maurice et al. 1989

(Luck & Lambert 1992). Fig. 2a gives an example of the behaviour of the abundance of Fe I lines as a function of their excitation potential for the final temperature chosen for the star PMMR 145.

– **the surface gravity log**g was derived from the ionisation equilibrium: we required that the iron abundance deduced from neutral and ionised species should be the same.
– **the microturbulent velocity** v_t was derived asking that the Fe I lines with small and large equivalent widths should give the same abundance. The uncertainty on this parameter is of the order of 0.5 km s^{-1} . Fig. 2b gives an example of the behaviour of the abundance of Fe I lines as a function of their equivalent width for the final v_t adopted for the star PMMR 145.

Galactic comparison star: Arcturus

As a Galactic reference, we analysed Arcturus, a well studied mildly metal poor K giant (see for example Peterson et al. 1993), for which M. Bessell kindly provided the spectrogram and the measurements of equivalent widths for iron, titanium and silicon. The closeness of the effective parameters of Arcturus and our program stars also enabled us to use it as a Galactic comparison (or "zero-point") for the abundance of individual elements: for elements only represented by a small number of lines, we used the spectrum of Arcturus to derive the abundance of the element *using the same lines as our program stars* to ensure the correctness of the physical parameters of the lines.

We also performed the analysis of the iron lines of Arcturus to determine its model atmosphere in the same way as with our program stars, and found an effective temperature of 4400 K, a gravity of 2.0 dex and microturbulent velocity of 1.5 km s^{-1} . Within the determination errors, these values are in good agreement with the study of Peterson et al. (1993) who found the best fitting model for $T_{\rm eff}$ =4300 K, log g =1.5 dex and v_t =1.7 km s^{-1} (by fitting the observed flux distribution). In fact, the Peterson values also give an acceptable agreement to our criteria, given that they are well within the expected intrinsic uncertainty of the method. Therefore, in the rest of the paper we shall discuss the abundances of Arcturus analysed with the parameters given by Peterson et al. (1993). Unfortunately, no comparison with equivalent width is possible.

The iron abundance that we obtain for this star from the analysis of the measurements of Bessell's spectrogram, Peterson's effective parameters and Plez's models ([Fe/H] = –0.51 dex) is the same as Peterson et al. found. But the overabundance of the light elements that we obtained is lower, which is partly due to the fact that they used a model with enhanced α-elements and therefore enhanced opacities, leading to the derivation of higher abundances from similar lines (part of the difference may also come from the difference between the Kurucz's and Plez's models).

Table 2. Physical parameters of the stars

star	$T_{\rm eff}$ K	log g dex	v_t km s^{-1}	[M/H] dex
PMMR 23	4200	0.2	4.0	–0.8
PMMR 27	4300	0.1	3.0	–0.6
PMMR 48	4300	0.3	3.5	–0.6
PMMR 102	4300	–0.2	3.5	–0.6
PMMR 144	4100	–0.7	3.5	–0.9
PMMR 145	4300	0.3	3.0	–0.6
Arcturus	4300	1.5	1.7	–0.6

Table 2 lists the adopted effective parameters for the program stars, together with the Galactic reference K giant Arcturus. In Fig. 3, we have plotted the empirical curve of growth of the Fe I together with the theoretical ones computed for the adopted atmospheric parameters for the star PMMR 145, as an illustration of the quality of the data and the models.

The star PMMR 23 displays a more scattered curve of growth because it is likely to have a faint red companion: we

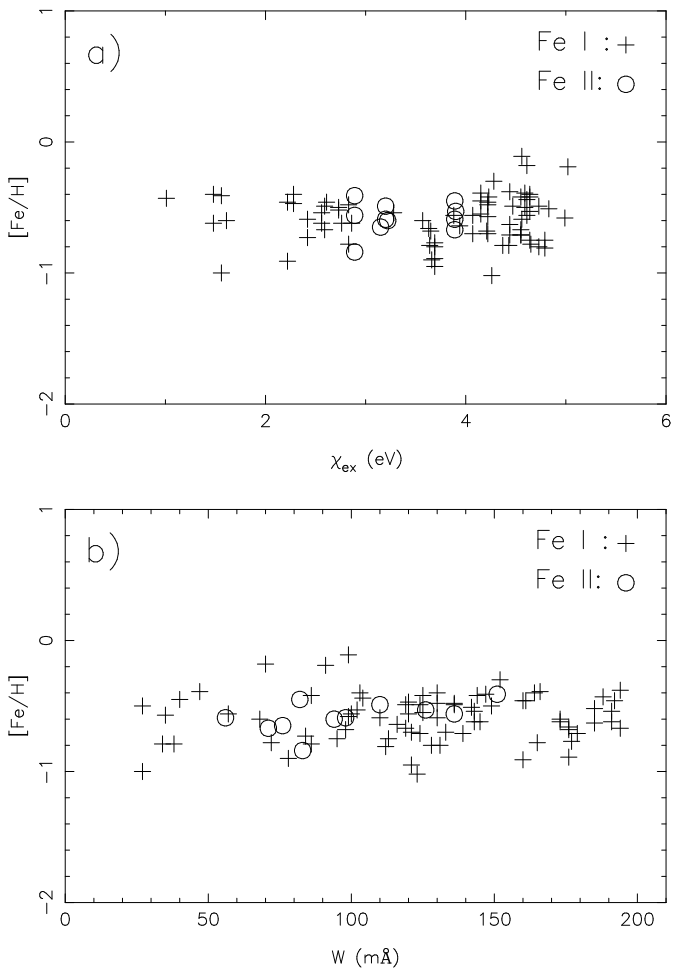

Fig. 2. a [Fe/H] abundance versus the excitation potential of the line for PMMR 145. The lack of correlation insures the excitation equilibrium and is a test of the good choice of effective temperature. **b** [Fe/H] abundance versus the equivalent width of the line. The lack of correlation is a test of the good choice of the microturbulent velocity.

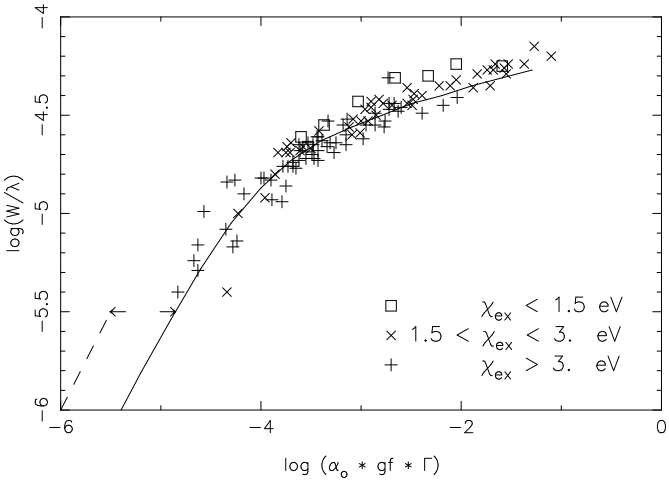

Fig. 3. Empirical and theoretical curves of growth of Fe I for the star PMMR 145. The abscissa is $X = log\alpha_{\odot} + loggf + log\Gamma(T_{eff}, g, M)$, where $\alpha_{\odot}$ is the abundance of the element in the Sun, gf the line transition probability and Γ (Cayrel & Jugaku, 1963) a function of the element M and of the stellar model. The horizontal distance between the dotted line (defined by $W/\lambda = X$) and the solid line (theoretical curve of growth) gives directly [Fe/H].

found from the red part of the spectrum that the lines' shape were slightly asymmetric. Because of this, we applied the atmospheric parameter determination on lines from the blue part of the spectrum. However, the resulting abundance should not be too much affected by the companion.

The star PMMR 144:

The temperature derived from the excitation equilibrium of this star was somewhat of a surprise to us since its $(B-V)$ color yielded a rather hot effective temperature (around 4500 K), and we found for this star a temperature not higher than 4100 K. So we reduced CCD *B,V,R* and *I* exposures (taken at the 1.54 m Danish Telescope at ESO, La Silla; kindly provided by E. Maurice) to derive the photometry of this star, using DAOPHOT package.The photmetry was reduced to the primary standards from Graham (1982) and stars from the cluster NGC 330 were used as secondary standards. From these new data we came to the conclusion that PMMR 144 has several faint blue companions within the aperture of the photometer used by Maurice et al. (1989). These companions, although faint (magnitudes 16 to 17), affected the measured color. Our new values for the photometry of this star are: V = 12.82 $(B-V)$ = 1.46 $(V-I)$ = 1.67 . The $(V-I)$ color is a very sensitive temperature indicator, moreover very little dependent on the surface gravity and the metallicity of the stars. The $(V-I)$ color yields a temperature of T_{eff} = 4000 K from the Plez' (Bessell et al. 1997) color indices, which is in close agreement with what is required from the excitation equilibrium of the Fe I lines.

4. Results

The individual line abundances for each star are listed in the Appendix. The mean abundance for each element are listed in Table 3 for each of the program stars.

4.1. Abundance uncertainties

The main sources of errors in the derived abundances may come in turn from three different sources: the measurement of the lines (equivalent widths or synthetic spectrum fitting), oscillator strengths (*gf*) of the lines and the uncertainty in the effective parameters of the stars.

The uncertainty in the equivalent widths of the lines are estimated from the Cayrel (1988) formula: $\Delta W_{\lambda} = \frac{1.6(\sigma\delta x)^{1/2}}{S/N}$, where S/N is the signal to noise ratio, δx is the pixel size (in Å) and σ is the standard width of the line. This estimation gives $\Delta W_{\lambda} \leq 5m$Å translating into an error of no more than 0.1 dex on the abundance of individual lines. But this line to line dispersion mostly cancels out when one considers the mean abundances of many lines so that this source of error may only dominate the abundances of species represented by few lines

Table 3. Abundances

Element	PMMR 23			PMMR 27			PMMR 48			PMMR 102		
	$[M/H]$	σ	N	$[M/H]$	σ	N	$[M/H]$	σ	N	$[M/H]$	σ	N
Na I	–0.55	0.09	3	–0.88	0.00	2	–0.62	0.04	2	–0.62	0.07	3
Mg I	–0.75	0.07	2							–0.40	0.14	2
Al I	–0.71	0.08	2	–0.85	0.07	2	–0.79	0.02	2	–0.90	0.00	2
Si I	–0.72	0.12	5	–0.90		1	–0.92	0.13	2	–0.71	0.22	5
Ca I	–0.72	0.39	4	–0.82	0.23	5	–0.81	0.35	5	–0.63	0.25	5
Sc II	–0.90	0.23	5	–0.98	0.11	2	–0.82	0.11	2	–0.90	0.23	6
Ti I	–0.61	0.23	7	–0.71	0.17	13	–0.61	0.17	9	–0.64	0.17	21
Cr I	–0.87	0.36	3	–1.13	0.27	2	–0.99	0.21	3	–0.90	0.27	4
Fe I	–0.74	0.21	60	–0.67	0.24	45	–0.66	0.26	39	–0.72	0.22	48
Fe II	–0.70	0.19	10	–0.66	0.21	8	–0.59	0.27	8	–0.69	0.20	11
Ni I	–1.04	0.26	10	–1.09	0.18	9	–0.98	0.13	9	–1.07	0.14	13
Y II	–0.85	0.21	2							–0.90	0.09	3
(Ba II	*0.57*	*0.24*	*2*	*0.47*	*0.15*	*3*	*0.35*	*0.22*	*3*	*0.05*	*0.49*	*2)*
La II	–0.26	0.16	2	–0.06	0.20	2	–0.12	0.14	2	–0.20	0.14	2
Ce II	–0.49	0.10	4	–0.46		1	–0.45		1	–0.54	0.08	5
Nd II	0.07	0.13	3							–0.16	0.18	4
Eu II	–0.23		1	–0.25		1	–0.10		1	–0.35		1

Element	PMMR 144			PMMR 145			Arcturus		
	$[M/H]$	σ	N	$[M/H]$	σ	N	$[M/H]$	σ	N
Na I	–0.77	0.05	2	–0.91	0.03	3	–0.33	0.15	3
Mg I				–0.47	0.04	2	–0.11	0.14	2
Al I	–0.87	0.00	2	–0.70	0.07	2			
Si I	–1.07	0.12	2	–0.69	0.13	5	–0.34	0.06	11
Ca I	–0.92	0.40	4	–0.72	0.17	7			
Sc II	–1.25	0.14	2	–0.74	0.25	6			
Ti I	–0.79	0.15	7	–0.66	0.23	23	–0.37	0.14	62
Cr I	–1.23	0.35	3	–0.91	0.20	4	–0.78	0.17	5
Fe I	–0.92	0.24	28	–0.59	0.18	77	–0.46	0.14	132
Fe II	–0.81	0.19	7	–0.58	0.12	11	–0.57	0.17	9
Ni I	–1.24	0.11	8	–1.03	0.21	16	–0.56	0.11	9
Y II				–0.93	0.12	3	–0.50	0.11	2
(Ba II	*0.10*	*0.44*	*3*	*0.40*	*0.17*	*3*	*–0.76*	*0.14*	*2)*
La II	–0.82	0.18	2	–0.10	0.07	2	–0.47	0.14	2
Ce II	–0.90		1	–0.43	0.12	5	–0.51	0.14	5
Nd II				–0.10	0.19	4	–0.30	0.11	4
Eu II	–0.66		1	–0.20		1	–0.32*		1

* calculated from the equivalent width from Mäckle et al. 1975 W_{Eu}=35 mÅ

(e.g. Mg, Al, La and Eu). Moreover, owing to the large overlap of our spectra, we usually were able to average two independent measurements of the same line.

In fact, for elements represented by many lines in our spectra, the line to line abundance dispersion is usually dominated by uncertainties in the oscillator strengths (*gf*). Nevertheless, the differential abundances from one star to the other should be independent of *gf* uncertainties since we are using the same lines for all the program stars (i.e the difference of abundance from one star to the other is free of the errors on *gf*). In particular, comparing the program stars abundances to those of Arcturus (computed from the same lines) is more reliable than considering the absolute abundances.

The third source of error comes from the uncertainty in the effective atmospheric parameters of the stars and thus affects each star differently. But the ratios of abundances of one element to the other are less affected than the absolute abundances of each species. As iron is the best represented element, we will discuss the ratios of all the elements relative to iron: [X/Fe]. Table 4 lists the errors on the abundance ratios (abundance of each element relative to iron) for the star PMMR 145 resulting from a variation of the atmospheric parameters of the stars within the expected uncertainty for each parameter (namely ΔT_{eff} = ±200 K, $\Delta log(g)$ = ±0.3 dex and Δv_t = ±0.5 km s^{-1}). However, since the gravity determination is closely linked to the temperature adopted for the star, a variation of +200 K in $T_{\rm eff}$ should not be considered alone, but

Table 4. Influence of the effective parameters uncertainties in the abundance ratios of PMMR 145. The table lists the abundance (relative to iron) changes Δ [X/Fe] for each element upon varying the atmospheric parameters of the star within the expected uncertainty range. The fist line gives the resulting shift in the mean iron abundance [(Fe I+Fe II)/H]. The last column is the square root of the sum of the square of columns 1 to 3 (see text).

El.	$\Delta log(g)$	Δv_t	$\Delta T_{eff}, \Delta log(g)$		$\sqrt{\sum \Delta^2}$
	+0.3 dex	+0.5 km/s	-200 K, -0.6 dex	+200 K, +0.6 dex	1,2,3
Fe_{mean}	0.08	–0.12	–0.11	0.13	0.18
Na I	–0.11	0.07	–0.03	0.01	0.13
Mg I	–0.09	–0.05	–0.01	0.02	0.10
Al I	–0.09	0.11	–0.03	0.00	0.15
Si I	–0.04	0.08	0.09	–0.06	0.13
Ca I	–0.10	0.00	–0.07	0.07	0.12
Sc II	0.05	–0.01	–0.07	0.09	0.09
Ti I	–0.09	0.03	–0.20	0.20	0.22
Cr I	–0.10	0.04	–0.15	0.14	0.18
Fe I	–0.06	0.00	–0.06	0.06	0.08
Fe II	0.07	0.01	0.08	–0.05	0.11
Ni I	–0.05	0.02	–0.05	0.06	0.07
Y II	0.03	0.02	–0.06	0.08	0.07
La II	0.04	0.02	–0.16	0.18	0.17
Ce II	0.12	–0.06	–0.21	0.25	0.25
Nd II	0.11	–0.09	–0.22	0.24	0.26
Eu II	0.05	0.06	–0.10	0.10	0.13

together with a shift in gravity by around +0.6 dex. Considering this, one can see that the final errors seldom exceed 0.1 dex for elements determined from lines with excitation potential close to those of the iron lines; for elements with low excitation potential such as Ti and La, the error can be as high as 0.2 dex. The most drastic effects are triggered by temperature changes, whereas gravity or microturbulence alone only accounts for a general shift in absolute abundances, leaving the abundance ratios very little affected. The last column of the table gives an estimate of the "global" errors due to effective parameters uncertainties, calculated as the square root of the sum of columns 1 to 3 to the square ($\sqrt{\sum \Delta^2}$ where Δ is the error listed in col. 1,2,3).

In short, we conclude that the typical errors in the determination of the effective parameters of the stars are likely to produce overall shifts in the absolute iron abundance of ≤ 0.15 dex, and errors on the abundance ratios around 0.10 (and seldom up to 0.2 dex where low excitation potential lines are concerned).

Note about effective gravities:
Gravities may be calculated from the mass,luminosity and temperature of the stars via the formula:

$$log(\frac{L_*}{L_\odot}) = log(\frac{M_*}{M_\odot}) + 4log(\frac{T_*}{T_\odot}) - log(\frac{g_*}{g_\odot}) \quad (1)$$

Assuming a mass of $10M_\odot$ for these stars (reasonable value, see Schaller et al. 1993), the gravities calculated from this formula exceed those derived from the ionisation equilibrium of Fe lines by 0.1 to 0.7 dex, as is generally observed in cool supergiants because of NLTE effects resulting in overionisation (Pilachowski et al. 1983, Spite et al. 1991). The choice of using the gravity determined by ionisation equilibria enables one to artificially compensate for the overionisation in a LTE model, and thus avoid deriving systematically low abundances from neutral species.

5. Discussion

5.1. Homogeneity

The mean iron abundance that we found for the six program K supergiant stars is $\overline{[Fe/H]}$=–0.69 $\pm$ 0.10 dex. This mean value agrees very well with previous determinations of iron abundances in the SMC, from F supergiant stars (LL92 found –0.6 dex, RB89 deduced –0.65$\pm$0.2 dex and SSF89 had –0.65$\pm$0.2 dex), and main sequence B stars (Rolleston et al. 1993 derived a metallicity of –0.8 dex from four B stars).

But unlike these previous studies, the program stars deviate very little from the mean, apart perhaps for the star PMMR 144 (see below). Given the expected uncertainty which may affect the star-to-star abundance scatter (namely, the errors in effective parameters determination), the expected star-to-stardeviations should be of the order of 0.15 dex. The observed dispersion among the program stars is of the same order, giving a hint of a very small variation in the chemical composition among the stars. One way to disentangle the errors due to the physical data (namely the *gf* values) from the real star-to-starscatter is to look at the differential abundances from star-to-star for each single line. The average star-to-star scatter obtained in this way for iron lines is 0.14 dex, and this holds for most other elements. This is again compatible with what may be expected from the atmospheric parameter uncertainty (which in this case adds to the error on equivalent width determination). Pagel et al. (1978) were the first to point out the strong abundance homogeneity found among the H II regions of the SMC (they found *no evidence* of a gradient with position in the SMC). But the previous studies of stars (RB89, LL92) gave somewhat more dispersed results ($\sigma \approx 0.17$). The present work thus reconciles the homogeneity found from H II regions and stars (i.e. objects of similar ages).

The structure of the SMC is somewhat lumpy: according to Martin et al. (1989), the H I gas is split into four kinematic components. Most of the young stellar population is associated with the two main gas components referred to as VH (high velocity) and VL (low velocity) components. Following Martin et al. (1989), the majority of our stars (4) are associated with the VH component, whereas PMMR 23 belongs to VL and PMMR 144 has a radial velocity falling in between the characteristic velocities for the VL and VH components and is hence classified as not associated with any of the gaseous components. The four stars associated with the VH component (mean

$\overline{[Fe/H]_{VH}}$=–0.64 ± 0.05 dex) and the star PMMR 23 associated with VL ($[Fe/H]_{PMMR\ 23}$=–0.72 dex) have very similar abundances, so there is no evidence for an abundance difference between these two kinematic components, although the statistics of our sample does not enable one to draw any definite conclusion.

The case of PMMR 144:
This star happens to be the most metal-poor of our sample, departing from the mean abundance by 0.16 dex which is barely significant. But it is worth pointing out that in addition, PMMR 144 is the only star of our sample which does not show any noticeable enhancement of the heaviest elements (La and Eu), enhancements which seems to be the characteristic of young stars in both Clouds (cf. Sect. 5.6).

Could it be that this star in fact belongs to the halo of our Galaxy ? Its radial velocity (179.7 km s^{-1}) is compatible with the kinematics of the halo, and its V magnitude, at characteristic halo distances, would mean that it is a low-mass star. In fact, using the relation (1) between the mass, luminosity, temperature and gravity of a star, we may infer the luminosity difference between a SMC supergiant (with the same T$_{\rm eff}$ and log g as PMMR 144) with a mass of $10M_{\odot}$ and a low-mass Galactic halo star of $0.8M_{\odot}$ (with the same T$_{\rm eff}$ and log g). This difference would be only a luminosity 2.7 magnitudes higher for the $10M_{\odot}$ star than for the $0.8M_{\odot}$. If the distance modulus of the SMC is taken to be 18.7, then the $0.8M_{\odot}$ PMMR 144 star would be 2.7 magnitude closer to us, therefore at a distance modulus of 16, which would be also compatible with the membership to the halo of our Galaxy.
However, PMMR 144 does not show the typical α-elements enhancement (with respect to iron) expected for metal-poor halo stars (cf. Sect. 5.4). Moreover, it has been suggested by Bessell (1992) that for stars with similar effective gravities and temperature, the microturbulence increases with the mass of the star. PMMR 144 has a microturbulent velocity of 3.5 km s^{-1} , typical of the massive supergiants of the Clouds, whereas less massive objects with similar T$_{\rm eff}$ and log g (e.g. HD184711) has v_t below 2 km s^{-1} . This would argue strongly for PMMR 144 to be a Magellanic supergiant rather than a projected Galactic star.

If PMMR 144 is not taken into account, the star-to-star scatter around the mean abundance for each element decreases *slightly* for iron and other species ($\overline{[Fe/H]}$=–0.66 ± 0.06 dex), and *drastically* for the heavy elements La and Eu (cf. Sect. 5.6).

5.2. Lithium

We searched for the lithium line at 6707.8 Å in the program stars and found a line at the expected wavelength in all of our stars, compatible with abundances of lithium ranging from $log(N_{Li}/N_H+12 \approx 0.0$ to 0.5 dex (PMMR 145 and PMMR 27 showing $log(N_{Li}/N_H$ + 12 ≈0.5 dex). The lithium detection suggests that the stars are in their first crossing of the HR diagram. However, due to the nearby CN band, we shall discuss the Lithium abundance in a forthcoming paper on C,N and O elements.

5.3. The odd element Na

Sodium is an interesting element known to display anomalous overabundances in some evolved stars and attributed to a possible Ne-Na cycle in the star, the product of which would be dredged towards the surface by deep-mixing following the first dredge-up phase. Sodium is represented in our spectra by two to three lines. Depending on the star, the observed [Na/Fe] ratio ranges from –0.3 to +0.15 dex which is a rather large scatter compared to what is observed for other elements, and $\overline{[Na/Fe]}$=–0.03±0.19 dex. Could that be due to different mixing stages of the various stars ? It would be very interesting to check for a possible correlation of the sodium overabundance against the C/N ratio (C/N is strongly affected by the CNO cycle which enhances nitrogen and depletes carbon). In Arcturus, the same three sodium lines give an overabundance of sodium with respect to iron of [Na/Fe]=+0.18 dex.

5.4. α-elements

Titanium is the best represented species of this so-called α-elements group with 7 to 23 lines and does not appear to be overabundant ([Ti/Fe] ranges from -0.08 to +0.11 dex). Similarly, other α-elements that we were able to measure show close to solar $\overline{[\alpha/Fe]}$=–0.04±0.10 dex (where α stands for the mean of Mg,Si,Ca and Ti). Only magnesium could be slightly enhanced, but we were able to measure this element in only three stars. This is compatible with what was previously observed in hotter stars of the SMC ([α/Fe]≈0.1 dex, LL92, SSF89). In Fig. 4 we plotted the ratio of α-elements to iron for each of the program stars, together with the Arcturus values, joined by dotted lines. Note that the star PMMR 144 behaves similarly to the other SMC stars. As can be seen, Arcturus shows an enhancement of the α capture elements by 0.15 to 0.2 dex, whereas this is not observed in our stars: at similar metallicities, galactic halo stars (such as Arcturus) show an increase of [α/Fe] (increasing with decreasing [Fe/H]), whereas SMC stars do not. This solar-like α-elements ratio of SMC stars also supports the remark first made by LL92, that $[\alpha/Fe]_{SMC} < [\alpha/Fe]_{LMC}$, in contrast with the Galactic trend of increasing $[\alpha/Fe]$ with decreasing metallicity.

5.5. Iron peak elements

Among the Iron-peak elements, apart from the iron itself, we were able to measure the equivalent widths for only a few chromium lines, but measured 9 to 16 lines for nickel.

The nickel to iron ratios have been found to be sub-solar in all our stars. This effect ($\overline{[Ni/Fe]}$=–0.38±0.05 dex) is too large to be explained by abundance errors, since the stars' effective parameters have little influence on the [Ni/Fe] ratio (cf. 4). Moreover, to check the validity of the physical parameters of the lines, we derived the nickel abundance of Arcturus using the same lines as in the program stars, and found a normal [Ni/Fe] ratio of –0.05 dex. On the other hand, in the hotter supergiants of both Magellanic clouds several authors (RB89, SSF89, LL92, Paper I) found the nickel abundance to follow closely that

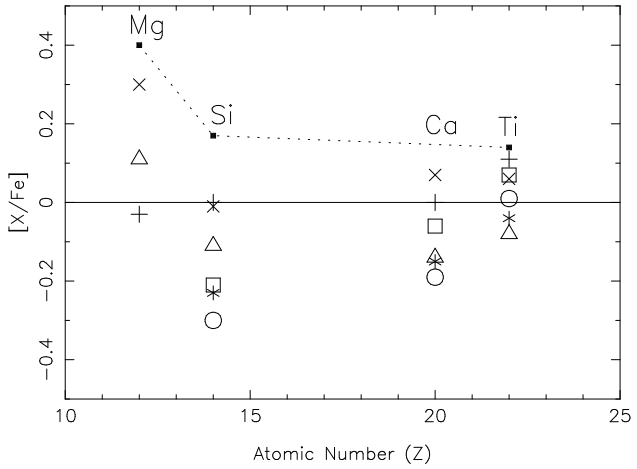

Fig. 4. Abundances of α-elements (relative to iron) versus atomic number, for the six SMC supergiant stars of our sample. Each star is represented by a different symbol. Arcturus is also plotted as a Galactic reference, represented by filled squares and joined with dotted lines. Note that the star PMMR 144, plotted as open squares behaves similarly to the Magellanic stars.

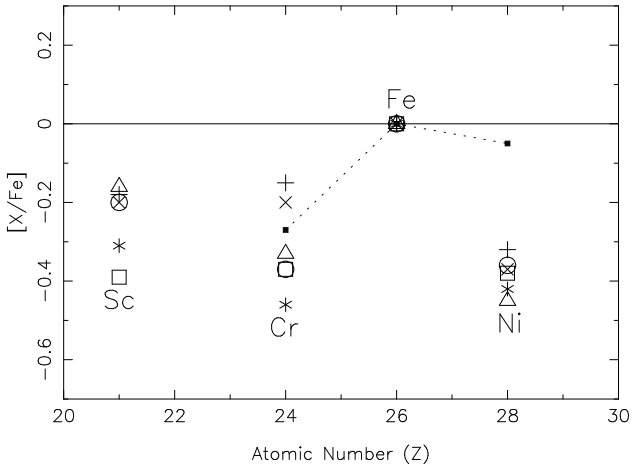

Fig. 5. Iron group elements abundances (relative to iron) versus atomic number, for the six SMC supergiant stars of our sample. Each star is represented by a different symbol. The star PMMR 144 is plotted as open squares. Arcturus is also plotted as a Galactic reference, represented by filled squares and joined with dotted lines. The star PMMR 144 is plotted as open squares and does not differ from the other Magellanic stars.

of iron ([Ni/Fe]$\approx$ 0), as may be expected from nucleosynthesis. But many nickel lines are weak in the hotter F supergiants and not measurable, so that the Ni abundance derived from the cooler stars should be more reliable; it is to be noted that Spite et al. (1991) found a similar over-deficiency of nickel with respect to iron in the cool stars of the young SMC cluster NGC330.
In our Galaxy, Edvardsson et al. (1993) showed that the nickel abundance in the disk stars follows very closely that of iron. In more metal poor stars, data are more scattered, but there is still no evidence for a deviation of nickel with respect to iron (e.g. Norris et al. 1993, Peterson et al. 1990, Gratton & Sneden 1991). It is also interesting to compare the SMC to the giant globular cluster Omega Cen , which shows clear signature of self-pollution and to 47 Tuc which has a metallicity similar to the SMC . However, in the Galactic giant globular cluster ω-Centauri, the situation is not clear: Norris & Da Costa (1995) found a over-deficiency of nickel, mild for the most metal-rich stars of the cluster, and stronger for the most metal poor ones (with an increased scatter as well); On the contrary, other authors (e.g. Smith et al. 1990, François et al. 1988) do not find any evidence for a trend. Finally , in the mildly deficient cluster 47 Tuc, D'Odorico et al. (1985) found a slight overabundance of nickel relative to iron (0.15 dex), not confirmed by Norris & Da Costa (1995).
The low nickel abundance found in our SMC K supergiants is therefore quite surprising, however, it has been sometimes found in some stars of old globular clusters.

Chromium, represented by only two to four lines ,also appears underabundant with respect to iron ($\overline{[Cr/Fe]}$=–0.31$\pm$0.12 dex. However, in this case, Arcturus also appears overdepleted by [Cr/Fe]=–0.27 dex (using the same four lines), so the program stars' underabundance may not be significant.

Scandium is also overdepleted, but this element is affected by hyperfine structure and although we took this effect into account, the resulting abundance may not be very reliable also due to an uncertainty in the *gf* values. In addition, this element is an odd element, and the odd-even effect is known to be somewhat enhanced in Galactic metal-poor stars (Arnett 1971; Truran & Arnett 1971; Primas et al. 1994) : this should be true also in the Magellanic Clouds.

In Fig. 5 we plotted the ratio of iron-group elements to iron for each of the program star, together with the Arcturus values, joined by dotted lines.

5.6. Heavy neutron capture elements

Among the heavy neutron-capture elements (*s*- and *r*- process), we were able to measure lines of yttrium, barium, lanthanium, cerium, neodymium and europium. In Fig. 6 we plotted the ratio of neutron-capture elements to iron for each of the program star, together with the Arcturus values, joined by dotted lines. The solid line represents the mean for the program stars, *PMMR 144 excluded*.

In all of our stars, except for PMMR 144, the heavier *s*- and *r*- process elements (namely La, Ce, Nd and Eu) are found to be significantly overabundant ($\overline{[s\&r/Fe]_{5stars}}$=+0.41$\pm$0.04 dex where $s\&r$ stands for the mean of La, Ce, Nd and Eu abundances, whereas $[s\&r/Fe]_{PMMR144}$=+0.07 dex). Using the same lines[1] , Arcturus shows only a small enhancement

[1] Unfortunately, the profile of the europium line at 6645Å could not be measured due to a lack of spectrum coverage in this wavelength range, but its equivalent width is available elsewhere in the literature. This element is affected by hyperfine structure; however, the 6645Å line is weak in Arcturus (W=35 mÅ) so that the HFS should not affect

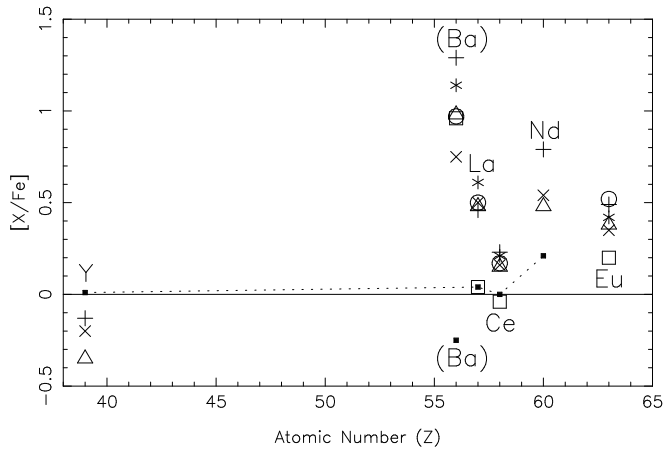

Fig. 6. Heavy elements abundances (relative to iron) versus atomic number, for the six SMC supergiant stars of our sample. Each star is represented by a different symbol. Arcturus is also plotted as a Galactic reference, represented by filled squares and joined with dotted lines. Note that the star PMMR 144, plotted as open squares, has abundances similar to Arcturus, significantly lower than the rest of the sample.

($[s\&r/Fe]_{Arcturus}$=+0.11 dex, where $s\&r$ is the mean of La, Ce and Nd calculated from Bessell's spectrum, and W_{Eu} is from Mäckle et al. 1975), comparable to the enhancement ($[s\&r/Fe]$ ≈+0.2 dex) found in Galactic F and G dwarfs with [Fe/H]=-0.5 dex (Woolf et al. 1995).
On the other hand, the lighter *s*- process element Y is found to be slightly depleted with respect to the solar [Y/Fe] ratio.
The strong enhancement of the heavier *s*- and *r*- process elements, and the normal abundance of lighter neutron capture elements such as Y found from previous studies of hotter stars of the SMC (RB89, LL92, SSF89), is therefore confirmed here.

Note: Barium abundance is rather poorly determined: in these stars, the Ba lines are very strong (300<W<700mÅ) and thus very much affected by damping and microturbulence (in Table 4 the effect of a microturbulent velocity change of 0.5km s^{-1} would be of 0.35 dex on the [Ba/Fe] ratio). Such strong lines were generally excluded from our analysis. Only because barium is an interesting indicator of heavy elements dominantly produced through *s*- process, did we include it in Table 3 (*in italics*). In addition, the excitation potential of these lines are very low (0.6 to 0.7 eV), which makes the abundance sensitive to temperature uncertainties. Therefore, the very strong Ba overabundance found here ($\overline{[Ba/Fe]}_{6stars}$=+1.01±0.18 dex) is questionable and should only be considered as an indication rather than a true numerical value. Considering this, we did not include barium in further discussion. It is furthermore to be noted that following RB89, the barium abundance in SMC F supergiants is [Ba/Fe]≈–0.2 dex whereas SSF89 found [Ba/Fe]≈+ 0.2 dex.

very much the derived abundance, at variance with the SMC supergiants for which the line is stronger (W≈100mÅ) and the abundance derived from the equivalent width is ≈0.15 dex higher than with the HFS taken into account.

The chemical evolution connection and comparison to the LMC:

The *r*- process elements are thought to be mainly produced in supernovae Type II of moderate mass (M ≈8$M_\odot$; Cowan et al. 1991, Mathews et al. 1992), whereas the *s*- process elements are likely to be produced in He burning shells of AGB stars of intermediate mass (the so-called *s*- process *main* component) and the *s*- process elements lighter or up to Y could be also partly produced by the *s*- process *weak* component (Prantzos, 1990), in the core of He burning of massive stars (M >11$M_\odot$).
In all the stars analysed so far in the Magellanic Clouds, the elements heavier than barium were found to be reinforced: the heavy *s*- and *r*- processed elements to iron ratio [$s\&r$/Fe] is around +0.3 dex in the LMC and +0.5 dex in the SMC (+0.4 dex in the present study). The ratio of elements considered as "pure" *r*- process (Eu) to elements which are a mixture of *s*- and *r*- process elements (La, Ce, Nd) is very similar to the solar value (e.g $log\epsilon(\mathrm{La})_{SMC} - log\epsilon(\mathrm{Eu})_{SMC} \approx log\epsilon(\mathrm{La})_\odot - log\epsilon(\mathrm{Eu})_\odot$).
Simultaneously, the *s*- process elements somewhat lighter (Y, Zr, etc..) seem to have a solar [*s*/Fe] ratio. There is therefore strong evidence that the enrichment by the products of the *r*- process has been especially efficient in the LMC and even more in the SMC, which, in turn, would demand a high efficiency of the production by the moderate-mass SN II.
On the other hand, let us recall that the α-elements in both Clouds (produced by SN II) are *not enhanced* relative to iron in the SMC ([α/Fe]≃0, this paper), and slightly depleted in the LMC ([α/Fe]≃–0.2 dex). The α-elements are thought to be produced most efficiently in SN II supernovae descended from massive, short-lived stars. The α-element depletion on the LMC could be understood if the star formation rate occurred in two well-separated bursts (Gilmore & Wise 1991), as suggested by the bi-modal distribution of the age of clusters in the LMC. However, the SFR in the Small Cloud appears (from the cluster distribution, CDM, etc..) to have been smoother over time so the α-elements to iron ratio should be higher than in the LMC. Thus, the α-element to iron ratio in both Magellanic Clouds may possibly be understood with an IMF similar to the Galactic one. But then, should not the *r*- process elements to iron ratio be slightly under solar in the LMC and solar in the SMC ?

In our Galaxy, the metal-poor stars also show an enhancement of *r*- process elements with respect to iron. For stars with metallicity ≥–2.5 dex, this ratio follows the oxygen to iron ratio (and [α/Fe]), going up to ≃0.5 dex for stars of metallicity ≃–2 dex (e.g. Woolf et al 1995 for Galactic Disk dwarfs). This correlation shows that the *r*- process is likely to occur at the same site that produce the oxygen and α-elements: Supernovae Type II. Furthermore, for more metal-poor stars (≃–3 dex), the [α/Fe] ratio remains on a plateau while the *r*- process elements decrease (Gratton & Sneden, 1994; Mc William et al. 1995), owing to their being produced by less massive, hence longer-lived, stars. In the Magellanic Clouds, it is thus far more tricky

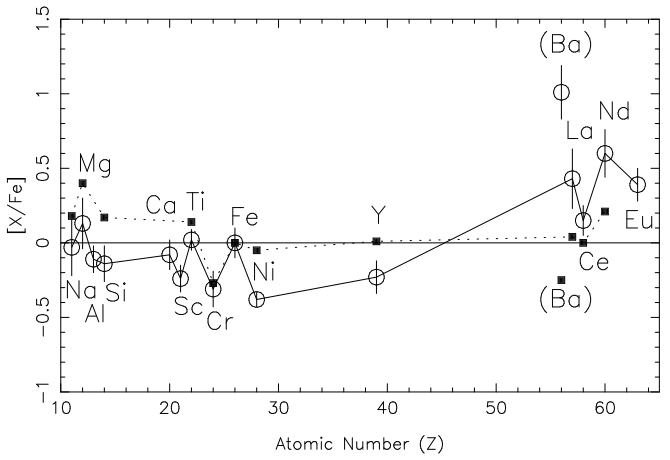

Fig. 7. The mean abundance (relative to iron) of the nine SMC supergiant stars of our sample is plotted versus atomic number (open circles), for all the measured elements. The error bar is the one-sigma dispersion over the sample. Arcturus is also plotted as a Galactic reference, represented by filled squares and joined with dotted lines.

to account *both for the pattern of* α*-elements and the heavy elements* at the same time: *r*- process elements are enhanced although they come from the same sites as α-elements, which are not enhanced. To explain such a pattern of abundances one needs either to account for a greater number of moderate-mass SN II versus high-mass SN II (via a flatter IMF), or to appeal to galactic winds (driven by the high-mass SN II) expelling more efficiently the products of massive SN II compared to those of the less massive ones, as proposed by Lambert (LL92). The first explanation has a major drawback: from cluster studies, there has been no evidence for an IMF different in the Clouds than in our Galaxy (e.g. Mateo 1993).

Could it be that the *main* component *s*- process is in fact responsible for a great proportion of the heavier elements ? As noted above, is seems from the data available that the relative abundance of elements heavier than Ba are compatible with the solar pattern (e.g. La/Eu, Nd/Eu or Ce/Eu). But a stronger contribution of the *s*- process cannot be ruled out. One would then have to account for the solar [Y/Fe] ratio (Y being an s-process element).

A better understanding of the sites of production of heavy neutron process elements is definitely needed to conclude this particular point. Obtaining reliable data for barium in the MCs would be of great help in disentangling the various processes.

6. Summary and conclusion

In Fig. 7, the mean [X/Fe] abundance for the six stars of our sample is plotted against atomic number (open circles joined by a solid line), together with the Arcturus values, joined by dotted lines. The error bar corresponds to the one sigma dispersion of the sample of the six SMC stars. The main effects which can be seen from this work are the following:

1. The mean iron abundance of the young population is confirmed to be around -0.7 dex. This value is compatible with previous studies of warmer supergiants (F stars) and with the analysis of B stars by Rolleston et al. (1993). 2. The scatter around the mean iron abundance is comparable with the expected error due to uncertainties in the effective parameters of the stars, so that there is no evidence of spread in abundance across various regions of the Cloud. This small dispersion holds for most elements. The data are even compatible with a very uniform metallicity for the K supergiants, implying a thorough mixing of the matter which formed the supergiants. A similar result was obtained for F supergiants in the LMC (Hill et al. 1995). Further, this is in agreement with the small abundance scatter among the H II regions within each Cloud (Pagel et al. 1978; Russell & Dopita 1990)

3. Sodium is not strongly enhanced in these stars and seems to vary from star to star.

4. At variance with metal-poor stars in our Galaxy (represented here by Arcturus), the so-called α-elements do not seem to be enhanced: only Mg could be slightly enhanced. This also confirms what was observed by previous studies of F supergiants: α-elements are more abundant (relative to iron) in the LMC than in the SMC.

5. Nickel displays a noticeable depletion with respect to iron ([Ni/Fe]≈–0.3 dex), at variance with what is found in the SMC F supergiants and in Arcturus.

6. Except for PMMR 144, the *s* and *r* process elements heavier than Ba are strongly enhanced in all of our stars ($\overline{[s\&r/Fe]_{5stars}}$=+0.41±0.04 dex where $s\&r$ stands for the mean of La, Ce, Nd and Eu), as previously found from F stars in both Clouds (enhanced by respectively 0.3 and 0.5 dex in the LMC and SMC).

Since the abundance determination in supergiants is always a difficult process owing to the very extreme atmospheres one is dealing with (possible NLTE effects, etc...), it is indeed very nice to find that the analysis of stars with different temperature (namely F from previous studies and K in the present paper) yields the same results concerning both the absolute iron abundance and the abundance ratios characteristic of the Magellanic Clouds (such as heavy elements enhancement, α-elements). The abundance of the light elements C, N, and O will be published elsewhere (Hill & Barbuy 1996) with further discussion of the implications of the relative abundances of elements on chemical evolution.

Acknowledgements. We thank M. Bessell for the use of his very useful and good quality high resolution Arcturus spectrum and for discussion about the color-temperature relation. We acknowledge E. Maurice for kindly lending us the CCD data for the photometry of PMMR144. We also thank B. Plez for communicating his most recent yet unpublished models.

Appendix

In Table 5, we give all the lines that we used in the analysis of our SMC K supergiants. The first four columns give respectively: the central wavelength of the line in Å, the element and

Table 5. Lines used in the analysis of our SMC K supergiants: **(1)** central wavelength of the line in Å, **(2)** element and its degree of ionization (1 for neutral and 2 for ionized species), **(3)** the excitation potential in eV, **(4)** line transition probability in log scale ($log(gf)$); columns **(5)** through **(14)** give, for each of the six SMC stars, the equivalent width (in mÅ) and the resulting abundance ([M/H], abundance in log scale, normalized to the Sun) for the line.

λ	El.	χ_{ex}	log gf	PMMR 23		PMMR 27		PMMR 48		PMMR 102		PMMR 144		PMMR 145	
				W	[X/H]	W	[X/H]	W	[X/H]	W	[X/H]	W	[X/H]	W	[X/H]
(Å)		(eV)		(mÅ)		(mÅ)		(mÅ)		(mÅ)		(mÅ)		(mÅ)	
5682.65	Na I	2.10	-0.71		-0.65					*136*	-0.58			*128*	-0.93
6154.23	Na I	2.10	-1.61	*99*	-0.50	*35*	-0.88	*75*	-0.65	*60*	-0.70	*58*	-0.80	*47*	-0.93
6160.75	Na I	2.10	-1.30	*135*	-0.50	*71*	-0.88	*106*	-0.60	*103*	-0.58	*84*	-0.73	*70*	-0.88
5528.42	Mg I	4.34	-0.25		-0.80				-0.20		-0.30				-0.50
5711.09	Mg I	4.34	-1.60		-0.70				-0.65	*194*	-0.50			*174*	-0.45
6696.03	Al I	3.14	-1.45	*56*	-0.77	*30*	-0.90	*42*	-0.80	*34*	-0.90	*50*	-0.87	*47*	-0.75
6698.67	Al I	3.14	-1.78	*60*	-0.65	*31*	-0.80	*35*	-0.77	*21*	-0.90	*28*	-0.87	*33*	-0.65
5665.56	Si I	4.92	-1.94	72.0	-0.65					71.0	-0.62			51.0	-0.80
5666.69	Si I	5.61	-1.74	28.0	-0.54					36.0	-0.40			29.0	-0.49
5690.43	Si I	4.93	-1.75	73.0	-0.82					67.0	-0.85			80.0	-0.63
5793.08	Si I	4.93	-1.91	60.0	-0.80			39.0	-1.01	44.0	-0.97	33.0	-1.16	51.0	-0.82
5948.55	Si I	5.08	-1.17	123.0	-0.77	94.0	-0.90	106.0	-0.83	121.0	-0.72	95.0	-0.99	110.0	-0.69
5260.39	Ca I	2.52	-1.71	125.0	-0.51									70.0	-0.79
5261.71	Ca I	2.52	-0.47							198.0	-0.76			184.0	-0.77
5867.57	Ca I	2.93	-1.58	95.0	-0.39	37.0	-0.82	63.0	-0.54	70.0	-0.41	77.0	-0.51	63.0	-0.51
6161.30	Ca I	2.52	-1.16			152.0	-0.62	176.0	-0.57	189.0	-0.40	158.0	-0.88	166.0	-0.50
6169.04	Ca I	2.52	-0.58	195.0	-1.27	150.0	-1.22	178.0	-1.13	187.0	-1.00	159.0	-1.46	175.0	-0.99
6455.61	Ca I	2.52	-1.30	180.0	-0.70	133.0	-0.71	165.0	-0.56	158.0	-0.57	154.0	-0.83	129.0	-0.76
6499.65	Ca I	2.52	-0.77			187.0	-0.73							192.0	-0.69
6572.79	Ca I	0.00	-4.26					174.0	-1.24						
5239.82	Sc II	1.45	-0.66		-0.65						-0.50				-0.45
5318.36	Sc II	1.36	-2.26								-1.10				
5526.82	Sc II	1.77	0.20		-1.10						-0.80			*198*	-0.90
5640.99	Sc II	1.50	-0.95		-1.15						-1.05				-1.00
5669.04	Sc II	1.50	-1.02		-0.70										-0.40
6245.62	Sc II	1.51	-1.07	*156*	-0.90	*151*	-0.90	*160*	-0.75	*169*	-0.85	*149*	-1.15	*146*	-0.80
6604.60	Sc II	1.36	-1.17			*131*	-1.05	*151*	-0.90	*162*	-1.10	*150*	-1.35	*133*	-0.90
5043.59	Ti I	0.84	-1.72											180.0	-0.25
5045.41	Ti I	0.85	-1.79											137.0	-0.66
5087.06	Ti I	1.43	-0.79							159.0	-0.67			132.0	-0.86
5113.45	Ti I	1.44	-0.79							134.0	-0.88			116.0	-1.01
5295.78	Ti I	1.07	-1.65							138.0	-0.58			107.0	-0.81
5351.07	Ti I	2.78	-0.07							32.0	-0.75			11.0	-1.33
5390.01	Ti I	1.87	-1.06							96.0	-0.35			63.0	-0.68
5474.23	Ti I	1.46	-1.34							126.0	-0.44			128.0	-0.40
5490.16	Ti I	1.46	-0.95							163.0	-0.54			151.0	-0.57
5648.58	Ti I	2.49	-0.36	76.0	-0.63					42.0	-0.74			55.0	-0.63
5689.48	Ti I	2.30	-0.45	115.0	-0.52					69.0	-0.63			87.0	-0.49
5903.33	Ti I	1.07	-1.93	103.0	-0.93	63.0	-1.00	84.0	-0.86	69.0	-0.93	97.0	-1.06	84.0	-0.82
5918.55	Ti I	1.07	-1.60	181.0	-0.76	106.0	-0.96	157.0	-0.66	136.0	-0.77	179.0	-0.78	135.0	-0.74
5922.12	Ti I	1.05	-1.47			149.0	-0.77	188.0	-0.58	180.0	-0.61			154.0	-0.73
5941.76	Ti I	1.05	-1.54			149.0	-0.70			176.0	-0.58			171.0	-0.51
5965.84	Ti I	1.88	-0.50			134.0	-0.64	185.0	-0.35	166.0	-0.45	179.0	-0.65	167.0	-0.35
6064.63	Ti I	1.05	-1.89	180.0	-0.53	119.0	-0.62	138.0	-0.56	124.0	-0.61	169.0	-0.63	126.0	-0.57
6091.18	Ti I	2.27	-0.42	110.0	-0.68	66.0	-0.79	75.0	-0.76	76.0	-0.69	84.0	-0.90	75.0	-0.72
6126.22	Ti I	1.07	-1.33			179.0	-0.65			189.0	-0.70			190.0	-0.55
6554.24	Ti I	1.44	-1.25			131.0	-0.65	166.0	-0.50	129.0	-0.71	158.0	-0.85	134.0	-0.64
6556.08	Ti I	1.46	-1.17			166.0	-0.43			192.0	-0.33			167.0	-0.42
6599.11	Ti I	0.90	-2.01			139.0	-0.65	182.0	-0.45	148.0	-0.65	192.0	-0.69	147.0	-0.60
6743.13	Ti I	0.90	-1.65			154.0	-0.92	191.0	-0.78	163.0	-0.93			172.0	-0.79
6861.50	Ti I	2.27	-0.84			63.0	-0.47								
6996.63	Ti I	2.33	-1.11	81.0	-0.20										
5783.07	Cr I	3.32	-0.30	106.0	-0.75					80.0	-0.75			74.0	-0.82
5787.93	Cr I	3.32	-0.16	146.0	-0.59			88.0	-0.87	111.0	-0.61	102.0	-0.88	94.0	-0.76
6330.10	Cr I	0.94	-2.82			163.0	-0.94	191.0	-0.86	161.0	-1.05	179.0	-1.25	173.0	-0.86
6362.88	Cr I	0.94	-2.70	193.0	-1.27	132.0	-1.32	157.0	-1.23	157.0	-1.20	154.0	-1.57	147.0	-1.21
5031.92	Fe I	4.37	-1.80											34.0	-0.79
5054.65	Fe I	3.64	-2.11											86.0	-0.79
5090.79	Fe I	4.26	-0.64	157.0	-1.01					144.0	-0.87			123.0	-1.02
5159.07	Fe I	4.28	-0.97	168.0	-0.57					177.0	-0.17			152.0	-0.30
5242.50	Fe I	3.63	-1.20											176.0	-0.66
5253.03	Fe I	2.28	-3.96	161.0	-0.47									120.0	-0.47
5253.47	Fe I	3.28	-1.60							127.0	-1.46			191.0	-0.54
5285.13	Fe I	4.43	-1.69	38.0	-0.88					41.0	-0.72			38.0	-0.79
5364.88	Fe I	4.44	-0.16											194.0	-0.38

Table 5. (continuing).

λ	El.	χ_{ex}	$\log gf$	PMMR 23		PMMR 27		PMMR 48		PMMR 102		PMMR 144		PMMR 145	
				W	[X/H]	W	[X/H]	W	[X/H]	W	[X/H]	W	[X/H]	W	[X/H]
(Å)		(eV)		(mÅ)		(mÅ)		(mÅ)		(mÅ)		(mÅ)		(mÅ)	
5365.41	Fe I	3.57	-1.42	194.0	-0.92					192.0	-0.60			173.0	-0.60
5367.48	Fe I	4.44	-0.04							168.0	-1.04			185.0	-0.63
5373.71	Fe I	4.47	-0.93	133.0	-0.70					93.0	-0.87			124.0	-0.49
5379.58	Fe I	3.69	-1.55	152.0	-1.00					150.0	-0.75			121.0	-0.95
5398.29	Fe I	4.44	-0.75	145.0	-0.82					136.0	-0.68			124.0	-0.71
5473.91	Fe I	4.15	-0.95							153.0	-0.71			166.0	-0.39
5525.55	Fe I	4.23	-1.33	127.0	-0.70					121.0	-0.55			125.0	-0.42
5543.20	Fe I	3.69	-1.65	150.0	-0.94					129.0	-0.89			128.0	-0.80
5543.94	Fe I	4.22	-1.16	141.0	-0.77					124.0	-0.71			136.0	-0.48
5554.90	Fe I	4.55	-0.45	154.0	-0.92					143.0	-0.79			139.0	-0.71
5567.40	Fe I	2.61	-2.73							199.0	-0.64			192.0	-0.46
5618.64	Fe I	4.21	-1.41	123.0	-0.70					103.0	-0.68			98.0	-0.68
5633.95	Fe I	4.99	-0.47	101.0	-0.77					91.0	-0.71			99.0	-0.58
5638.27	Fe I	4.22	-0.90	159.0	-0.90					167.0	-0.56			160.0	-0.46
5775.09	Fe I	4.22	-1.15	116.0	-1.02					113.0	-0.86			121.0	-0.70
5778.46	Fe I	2.59	-3.61	133.0	-0.69					124.0	-0.53			119.0	-0.49
5806.73	Fe I	4.61	-1.00	107.0	-0.72			105.0	-0.59	103.0	-0.58	92.0	-0.81	100.0	-0.56
5809.22	Fe I	3.88	-1.76	138.0	-0.71			176.0	-0.13	116.0	-0.68	102.0	-0.98	120.0	-0.56
5816.38	Fe I	4.55	-0.72	184.0	-0.44			148.0	-0.54	154.0	-0.46	131.0	-0.81	144.0	-0.42
5916.26	Fe I	2.45	-2.95			192.0	-0.59					197.0	-1.04		
5983.69	Fe I	4.55	-0.78	168.0	-0.54					121.0	-0.74	116.0	-0.92	119.0	-0.67
5987.07	Fe I	4.79	-0.45	118.0	-0.95			112.0	-0.86	116.0	-0.80	105.0	-1.02	113.0	-0.75
6024.07	Fe I	4.55	-0.05	195.0	-1.05	172.0	-0.80	180.0	-0.92	194.0	-0.77	179.0	-1.06	179.0	-0.71
6027.06	Fe I	4.07	-1.25	147.0	-0.91	129.0	-0.75	137.0	-0.79	146.0	-0.70	173.0	-0.61	133.0	-0.70
6056.01	Fe I	4.73	-0.54	111.0	-1.01			123.0	-0.75	119.0	-0.77	109.0	-0.98	136.0	-0.49
6078.50	Fe I	4.79	-0.41	126.0	-0.94	97.0	-0.97	109.0	-0.93	117.0	-0.84	98.0	-1.13	112.0	-0.81
6079.02	Fe I	4.65	-1.05	91.0	-0.77	66.0	-0.85	82.0	-0.73	83.0	-0.70	79.0	-0.86	72.0	-0.78
6082.72	Fe I	2.22	-3.78	196.0	-0.64	176.0	-0.31	180.0	-0.45	179.0	-0.48	192.0	-0.65	161.0	-0.46
6089.57	Fe I	5.02	-0.95	83.0	-0.44	75.0	-0.36	86.0	-0.31	95.0	-0.20	80.0	-0.45	91.0	-0.19
6102.18	Fe I	4.83	-0.32			117.0	-0.79	140.0	-0.68	138.0	-0.69	123.0	-0.94	142.0	-0.51
6180.21	Fe I	2.73	-2.75			192.0	-0.46					189.0	-0.97	185.0	-0.52
6188.00	Fe I	3.94	-1.69	130.0	-0.80	116.0	-0.64			113.0	-0.75	120.0	-0.87	116.0	-0.64
6232.65	Fe I	3.65	-1.40	195.0	-1.00	165.0	-0.82	167.0	-0.96	193.0	-0.73	165.0	-1.19	176.0	-0.68
6240.65	Fe I	2.22	-3.37			151.0	-1.01	158.0	-1.07	146.0	-1.18			160.0	-0.91
6270.23	Fe I	2.86	-2.62	179.0	-1.04			166.0	-0.86	168.0	-0.85	185.0	-0.96	173.0	-0.62
6301.51	Fe I	3.65	-0.84			182.0	-1.20								
6302.50	Fe I	3.69	-1.26			166.0	-0.90	192.0	-0.82			166.0	-1.28	177.0	-0.77
6311.50	Fe I	2.83	-3.25	136.0	-0.76	121.0	-0.57	148.0	-0.43	139.0	-0.51	153.0	-0.66	130.0	-0.48
6392.54	Fe I	2.28	-4.11	173.0	-0.44	124.0	-0.47	159.0	-0.26	147.0	-0.38	166.0	-0.53	130.0	-0.40
6408.03	Fe I	3.69	-1.17			166.0	-1.01	177.0	-1.07	182.0	-1.04	193.0	-1.15	176.0	-0.89
6419.96	Fe I	4.73	-0.33	179.0	-0.71	118.0	-0.94	132.0	-0.91	157.0	-0.68	113.0	-1.21	131.0	-0.80
6475.63	Fe I	2.56	-2.90			196.0	-0.58							191.0	-0.62
6518.37	Fe I	2.83	-2.63	185.0	-1.06	145.0	-0.99	166.0	-0.92	172.0	-0.89	169.0	-1.19	165.0	-0.78
6575.04	Fe I	2.59	-2.79							197.0	-0.88			194.0	-0.67
6581.22	Fe I	1.48	-4.92	175.0	-0.81	173.0	-0.39	194.0	-0.35	170.0	-0.58			145.0	-0.62
6625.04	Fe I	1.01	-5.42	198.0	-0.86					172.0	-0.77			188.0	-0.43
6703.58	Fe I	2.76	-3.13	179.0	-0.73	132.0	-0.74	141.0	-0.75	132.0	-0.84	131.0	-1.12	143.0	-0.62
6710.32	Fe I	1.48	-4.99			127.0	-0.74	147.0	-0.66	140.0	-0.74	133.0	-1.15	164.0	-0.40
6739.52	Fe I	1.56	-5.02			157.0	-0.35	194.0	-0.16			159.0	-0.82	147.0	-0.41
6752.72	Fe I	4.64	-1.17			106.0	-0.38	132.0	-0.22	110.0	-0.42	129.0	-0.40	103.0	-0.40
6806.86	Fe I	2.73	-3.25	175.0	-0.70	138.0	-0.62	107.0	-0.95					149.0	-0.50
6810.27	Fe I	4.61	-1.17	108.0	-0.63	77.0	-0.71	87.0	-0.66					104.0	-0.44
6820.37	Fe I	4.64	-1.33	106.0	-0.44	74.0	-0.55	71.0	-0.61					86.0	-0.42
6828.60	Fe I	4.64	-1.06	142.0	-0.44	103.0	-0.52	111.0	-0.52					102.0	-0.53
6837.01	Fe I	4.59	-1.86	54.0	-0.43	41.0	-0.47	45.0	-0.44					47.0	-0.39
6839.84	Fe I	2.56	-3.51	172.0	-0.71	118.0	-0.78	135.0	-0.71					143.0	-0.54
6842.69	Fe I	3.66	-2.23	93.0	-0.98	60.0	-1.10	70.0	-1.02					78.0	-0.90
6843.66	Fe I	4.64	-0.91	93.0	-0.97	96.0	-0.75	103.0	-0.75					95.0	-0.75
6844.68	Fe I	1.56	-5.62	54.0	-0.86	34.0	-0.89	33.0	-0.91					27.0	-1.00
6851.65	Fe I	1.61	-5.44	110.0	-0.54	80.0	-0.51	89.0	-0.46					68.0	-0.60
6854.85	Fe I	4.59	-2.06	39.0	-0.40	17.0	-0.73							27.0	-0.50
6855.17	Fe I	4.56	-0.82	118.0	-0.97	123.0	-0.67	140.0	-0.62					130.0	-0.59
6855.72	Fe I	4.61	-1.77	94.0	-0.14	73.0	-0.15	71.0	-0.21					70.0	-0.18
6857.25	Fe I	4.07	-2.25	55.0	-0.73	44.0	-0.72	44.0	-0.74					57.0	-0.56
6860.33	Fe I	2.61	-4.20	81.0	-0.56										
6861.95	Fe I	2.42	-3.95			94.0	-0.74							110.0	-0.59
6862.50	Fe I	4.56	-1.61			98.0	-0.13							99.0	-0.11
6880.64	Fe I	4.15	-2.47			40.0	-0.45							40.0	-0.45
6898.31	Fe I	4.22	-2.33	30.0	-0.77	29.0	-0.67							35.0	-0.57
6911.52	Fe I	2.42	-4.05	151.0	-0.51	92.0	-0.66							84.0	-0.73
6916.69	Fe I	4.15	-1.48	150.0	-0.65	121.0	-0.59							125.0	-0.55

Table 5. (continuing).

λ	El.	χ_{ex}	$\log gf$	PMMR 23		PMMR 27		PMMR 48		PMMR 102		PMMR 144		PMMR 145	
				W	[X/H]	W	[X/H]	W	[X/H]	W	[X/H]	W	[X/H]	W	[X/H]
(Å)		(eV)		(mÅ)		(mÅ)		(mÅ)		(mÅ)		(mÅ)		(mÅ)	
6933.03	Fe I	4.19	-2.40	52.0	-0.45										
6988.53	Fe I	2.40	-3.59	178.0	-0.83										
6999.89	Fe I	4.10	-1.55	150.0	-0.66										
5284.11	Fe II	2.89	-3.24	135.0	-0.98					174.0	-0.53			151.0	-0.41
5325.56	Fe II	3.22	-3.43	110.0	-0.63					109.0	-0.71			94.0	-0.60
5425.26	Fe II	3.20	-3.35	95.0	-0.91					110.0	-0.82			110.0	-0.49
5991.38	Fe II	3.15	-3.74	84.0	-0.74	67.0	-0.87	76.0	-0.73	80.0	-0.91			76.0	-0.65
6084.11	Fe II	3.20	-4.02	68.0	-0.58	55.0	-0.70	58.0	-0.61	76.0	-0.62	55.0	-0.89	56.0	-0.59
6149.25	Fe II	3.89	-2.94			85.0	-0.50	102.0	-0.29	94.0	-0.62	90.0	-0.62	82.0	-0.45
6247.56	Fe II	3.89	-2.58	113.0	-0.65	109.0	-0.54	100.0	-0.68	127.0	-0.61	102.0	-0.84	98.0	-0.59
6416.93	Fe II	3.89	-2.87	93.0	-0.58	79.0	-0.66	91.0	-0.50	99.0	-0.65	79.0	-0.86	71.0	-0.67
6432.68	Fe II	2.89	-3.80	105.0	-0.81	91.0	-0.84	89.0	-0.85	121.0	-0.76	88.0	-1.13	83.0	-0.84
6456.39	Fe II	3.90	-2.27	178.0	-0.32	155.0	-0.26	176.0	-0.13	181.0	-0.33	157.0	-0.54	126.0	-0.53
6516.08	Fe II	2.89	-3.44	146.0	-0.79	119.0	-0.87	114.0	-0.94	127.0	-1.06	151.0	-0.82	136.0	-0.56
5032.73	Ni I	3.90	-1.17											28.0	-1.09
5082.35	Ni I	3.66	-0.45	117.0	-1.29					105.0	-1.22			99.0	-1.22
5102.97	Ni I	1.68	-2.72							173.0	-1.00			187.0	-0.56
5197.17	Ni I	3.90	-1.07											26.0	-1.25
5388.35	Ni I	1.93	-3.36	72.0	-1.16					73.0	-0.99			70.0	-0.98
5625.33	Ni I	4.09	-0.60							87.0	-0.77			80.0	-0.79
5805.23	Ni I	4.17	-0.52	62.0	-1.11					47.0	-1.19			51.0	-1.12
5847.01	Ni I	1.68	-3.36	157.0	-0.95	110.0	-1.01	129.0	-0.91	140.0	-0.85	140.0	-1.14	124.0	-0.86
6111.08	Ni I	4.09	-0.76	54.0	-1.08	41.0	-1.14	52.0	-1.01	45.0	-1.11	47.0	-1.20	45.0	-1.08
6175.37	Ni I	4.09	-0.48	102.0	-0.94			73.0	-1.08	68.0	-1.13	69.0	-1.24	68.0	-1.09
6314.67	Ni I	1.93	-1.88			186.0	-1.45							182.0	-1.47
6327.60	Ni I	1.68	-3.00			157.0	-1.00	188.0	-0.85	164.0	-1.10	178.0	-1.28	170.0	-0.84
6482.81	Ni I	1.93	-2.71			160.0	-0.92	182.0	-0.86	170.0	-1.01	179.0	-1.22	156.0	-0.94
6586.32	Ni I	1.95	-2.68	184.0	-1.16	139.0	-1.14	162.0	-1.04	157.0	-1.13	157.0	-1.42	141.0	-1.10
6598.61	Ni I	4.23	-0.90	23.0	-1.24	26.0	-1.10	24.0	-1.14	21.0	-1.22	36.0	-1.07	33.0	-0.96
6772.32	Ni I	3.66	-0.84	118.0	-1.08	80.0	-1.22	94.0	-1.13	86.0	-1.22	93.0	-1.33	85.0	-1.15
6850.44	Ni I	3.68	-1.92	68.0	-0.38	25.0	-0.83	28.0	-0.77						
5087.43	Y II	1.08	-0.20	*187*	-1.00					*192*	-1.00			*172*	-1.00
5289.82	Y II	1.03	-1.89							*27*	-0.85			*41*	-0.80
5402.78	Y II	1.84	-0.59	*90*	-0.70					*74*	-0.85			*65*	-1.00
5853.69	Ba II	0.6	-0.92	*124*	0.40	*410*	0.30	*338*	0.10	*352*	-0.30	*326*	-0.40	*342*	0.20
6141.72	Ba II	0.7	-		0.74		0.60		0.50		0.40		0.45		0.50
6496.93	Ba II	0.6	-			*308*	0.50	*559*	0.44			*600*	0.25	*415*	0.50
6320.43	La II	1.50	-1.86		-0.37		-0.20		-0.22		-0.30		-0.95		-0.15
6390.49	La II	0.32	-1.60	*182*	-0.14	*138*	0.08	*137*	-0.02	*161*	-0.10	*130*	-0.70	*135*	-0.05
5187.46	Ce II	1.21	0.13							*114*	-0.40			*94*	-0.35
5274.24	Ce II	1.04	0.15	*127*	-0.60					*126*	-0.55			*113*	-0.40
5330.56	Ce II	0.87	-0.36	*106*	-0.50					*93*	-0.60			*79*	-0.50
5468.39	Ce II	1.40	0.14	*83*	-0.50					*67*	-0.58			*55*	-0.60
6043.40	Ce II	1.21	-0.43	*70*	-0.35	*52*	-0.46	*46*	-0.45	*54*	-0.55	*49*	-0.90	*55*	-0.32
5293.17	Nd II	0.82	-0.10	*228*	0.20					*198*	0.10			*167*	0.15
5416.38	Nd II	0.86	-1.20	*80*	0.05					*50*	-0.28			*40*	-0.20
5431.54	Nd II	1.12	-0.57	*108*	0.00					*90*	-0.15			*77*	-0.05
5485.71	Nd II	1.26	-0.30	*112*	-0.05					*84*	-0.30			*58*	-0.28
6645.13	Eu II	1.38	0.18	*135*	-0.23	*112*	-0.25	*131*	-0.10	*134*	-0.35	*116*	-0.66	*109*	-0.20

* asterisks surrounding the equivalent width means that the corresponding abundance was determined by fitting the the line profile rather than using this equivalent width, due to a severe blend or to the hyperfine structure of the line.

its degree of ionization, the excitation potential in eV, the line transition probability in log scale ($log(gf)$). Then we give for each of the six SMC stars, the equivalent width (in mÅ) and the resulting abundance ([M/H], normalized to the Sun) for the line. Asterisks surrounding the equivalent width means that the abundance was determined by fitting the line profile rather than using this equivalent width, due to a severe blend or to hyperfine structure of the line.

References

Arnett, W.D., 1971, ApJ 166, 153

Bessell, M., 1992, in: ESO Workshop and Proceedings Proceeding 40: "High Resolution Spectrosocopy with the VLT", M.-H. Ulrich (eds.), p. 75

Bessell, M., Castelli, F., Plez, B., 1997, A&A (to be submitted)

Cayrel R., 1988, in: Impact of Very High S/N Spectroscopy on Stellar Physics, G. Cayrel de Strobel and M. Spite (eds.), Kluwer, Dordrecht, p. 345

Cowan, J.J., Thielemann, F.-K, Truran, J.W., 1991, Ann. Rev. A&A 29, 447

Delbouille L., Neven L., Roland G., 1973, Atlas Photometrique du Spectre Solaire, Institut d'Astrophysique de Liège.

Edvardsson, B., Andersen, J., Gustafsson, B., Lambert, D.L., Nissen, P.E., Tomkin, J., 1993, A&A 275, 101

Graham, J.A., 1982, PASP 94, 244
Gratton, R.G., Sneden, C., 1994, A&A 287, 927
Grieve G.R., Madore B.F., 1986, ApJS 62, 427
Holweger H., Müller E.A., 1974, Solar Phys. 39, 19
Hill, V., Andrievsky, S., Spite, M., 1995, A&A 293, 347 (Paper I)
Luck R.E., Lambert D.L.,1992, ApJS 79, 303 (LL92)
Mäckle, R., Holweger, H., Griffin, R., 1975, A&A 38, 239
Mateo, M., 1993, in: The GLobular Cluster-Galaxy connection, ASP Conf. 48
Mathews, G.J., Bazan G., Cowan, J.J., 1992, ApJ 391, 719
Maurice, E., Bouchet, P., Martin, N., 1989, A&AS 78,455
Mc William, A., Preston, G., Sneden, C., Searle, L., 1995 AJ 109, 2757
Meliani, M.T., Barbuy, B., Richtler T., 1995, A&A 304, 347
Pagel, B.E.J., Edmunds, M.G., Fosbury, R.A.E., Webster, B.L., 1978, MNRAS, 184, 569
Peterson, R., Dalle Ore, C., Kurucz, R., 1993, ApJ 404, 333
Plez B., Brett, J.M., Nordlund, A., 1992, A&A 256, 551
Plez, B., 1995, private communication
Prantzos, N., Hashimoto, M., Nomoto, K., 1990, A&A 234, 211
Prévot, L., Martin, N., Maurice, E., Rebeirot, E., Rousseau, J., 1983, A&AS 53, 255
Primas, F., Molaro, P., Castelli, F., 1994, A&A 290, 885
Russell S.C., Bessell M.S.,1989, ApJS 70, 865 (RB89)
Russell S.C., Dopita, M.A., 1990, ApJS 74, 93
Rolleston, W.R.J., Dufton, P.L., Fitzsimmons, A., Howarth, I.D., Irwin, M.J., 1993, A&A 277, 10
Schaller, D., Meynet, G., Maeder, A., Schaller, G., 1993, A&AS 98, 523
Spite F., Barbuy B., Spite M., 1993, A&A 272, 116
Spite F., Spite M., 1992, in: New Aspects of Magellanic Cloud Research, Baschek B., Klare G., Lequeux J. (eds.), Springer, Berlin, p313
Spite F., Richtler T., Spite M., 1991, A&A 252, 557
Spite M., 1990, 2nd ESO/ST-ECF Data Analysis workshop. ESO Conference and Workshop Proceedings No34, Baade D., Grøsbol P.J. (eds.), p125
Spite F., Spite M., François P., 1989a,A&A 210, 25 (SSF89)
Truran, J.W., Arnett, W.D., 1971, Astrophys. Space Sci. 11, 430
Tsujimoto, T., Nomoto, K., Yoshii, Y., Hashimoto, M., Yanagida, S., Thielemann, F.K., MNRAS 277, 945
Woolf, V.M., Tomkin, J., Lambert, D.L., 1995, ApJ 453, 660

This article was processed by the author using Springer-Verlag LaTeX A&A style file *L-AA* version 3.